570 *Biochemistry* **2010,** *49,* 570–581
DOI: 10.1021/bi9011308

BIOCHEMISTRY
including biophysical chemistry & molecular biology
Article

Antibodies Raised Against Chlamydial Lipopolysaccharide Antigens Reveal Convergence in Germline Gene Usage and Differential Epitope Recognition[†,‡]

Cory L. Brooks,[§,▽] Sven Müller-Loennies,[∥,▽] Svetlana N. Borisova,[§] Lore Brade,[∥] Paul Kosma,[⊥] Tomoko Hirama,[#] C. Roger MacKenzie,[#] Helmut Brade,*[,∥] and Stephen V. Evans*[,§]

[§]*University of Victoria, Department of Biochemistry and Microbiology, PO Box 3055 STN CSC, Victoria, BC, Canada V8P 3P6,* [∥]*Research Center Borstel, Leibniz Center for Medicine and Biosciences, Parkallee 22, D-23845 Borstel, Germany,* [⊥]*Department of Chemistry, University of Natural Resources and Applied Life Sciences, A-1190 Vienna, Austria, and* [#]*Institute for Biological Sciences, National Research Council Canada, Ottawa, ON, Canada K1A 0R6* [▽]*These authors contributed equally to this work.*

Received July 2, 2009; Revised Manuscript Received November 30, 2009

ABSTRACT: The structures of antigen-binding fragments from two related monoclonal antibodies have been determined to high resolution in the presence of several carbohydrate antigens raised against chlamydial lipopolysaccharide. With the exception of CDR H3, antibodies S54−10 and S73−2 are both derived from the same set of germline gene segments as the previously reported structures S25−2 and S45−18. Despite this similarity, the antibodies differ in specificity and the mechanism by which they recognize their cognate antigen. S54−10 uses an unrelated CDR H3 to recognize its antigen in a fashion analogous to S45−18; however, S73−2 recognizes the same antigen as S45−18 and S54−10 in a wholly unrelated manner. Together, these antibody−antigen structures provide snapshots into how the immune system uses the same set of inherited germline gene segments to generate multiple possible specificities that allow for differential recognition of epitopes and how unrelated CDR H3 sequences can result in convergent binding of clinically relevant bacterial antigens.

The bacterial family *Chlamydiaceae* is comprised of two genera, *Chlamydia* and *Chlamydophila*, with a total of four species, *C. psittaci*, *C. trachomatis*, *C. pneumoniae*, and *C. pecorum*, all of which are pathogenic and obligatory intracellular bacteria that cause a variety of diseases in both animals and humans (*1*). Antibodies against specific lipopolysaccharide (LPS[1]) structures are critical to the clinical diagnosis of chlamydial diseases in medicine. The LPS of *Chlamydiaceae* are highly immunogenic and contain a family specific epitope of the structure Kdo(2→8)Kdo(2→4)Kdo (Figure 1A, epitope G), where Kdo is 3-deoxy-α-D-*manno*-oct-2-ulosonic acid.

In addition, *C. psittaci* LPS contains the trisaccharide Kdo-(2→4)Kdo(2→4)Kdo (Figure 1B, epitope I) and the tetrasaccharide Kdo(2→8)[Kdo2→4]Kdo(2→4)Kdo (Figure 1C, epitope J) (*2*). Whereas Kdo(2→4)Kdo(2→4)Kdo also occurs in trace amounts in *C. trachomatis* and *C. pneumoniae*, the tetrasaccharide has so far been found only in *C. psittaci* and a panel of monoclonal antibodies (mAb) against both structures have been shown to differentiate between *C. psittaci* and the other chlamydiae using immunofluorescence (*3*).

Monoclonal antibodies against the family specific Kdo oligosaccharides exhibit a wide range of specificities and affinities (*3*−*10*). The structures of two such mAb named S25−2 and S45−18 (*9*, *11*) have provided valuable insights into the nature of inherited immunity and the role of germline gene segments in the antibody response to carbohydrate epitopes. Both antibodies were derived from the same set of germline V-gene segments, which produce antibodies that fold to give a binding pocket of conserved sequence that recognizes the terminal Kdo, together with a flexible binding groove that determines global specificity.

The adaptive immune response is mediated by antibodies, which serve to recognize foreign antigens and protect against pathogens. Despite the tremendous diversity in potential antigens, only a limited number of germline genes are available to generate antibodies in response to an immunogenic challenge (*12*). The diversity of the primary antibody repertoire can be further enhanced by somatic hypermutation, a process that is usually dependent on T-cell help (*13*); however, carbohydrate immunogens are usually unable to elicit T-cell help and thus antibodies directed against carbohydrates have a greater dependence on the primary germline gene recombination. Further, for the primary germline antibody repertoire to be effective in providing immunity, it must at the same time be highly specific yet adaptable to new antigenic challenges.

Although antibodies directed against specific protein antigens have been structurally characterized in detail (for reviews see refs (*14*, *15*)), the structures of relatively few carbohydrate specific antibodies have been determined (*9*−*11*, *16*−*21*). To fully explore the antibody response to carbohydrate antigens, we

[†]This work was supported in part by grants from the Natural Sciences and Engineering Research Council of Canada and the Michael Smith Foundation for Health Research (S.V.E.), the Deutsche Forschungsgemeinschaft grant SFB 470/C1 (S.M.L. and H.B.) and from the Austrian Science Fund FWF-grants P17407 and P19295 (P.K.).

[‡]The atomic coordinates and structure factors (codes) have been deposited in the Protein Data Bank, Research Collaboratory for Structural Bioinformatics, Rutgers University, New Brunswick, NJ (http://www.rcsb.org). S73−2: 3HZM (Kdo), 3HZK (Kdo2.4Kdo), 3HZY (Kdo2.4Kdo2.4Kdo), 3HZV (Kdo2.8Kdo2.4Kdo); S54−10: 3I02 (Kdo2.4Kdo2.4Kdo).

*To whom correspondence should be addressed. For H.B.: phone, 04537-188-474; fax, 04537-188-419; E-mail, hebra@fz-borstel.de. For S.V.E.: phone, 250-721-4548; fax: 250-721-8855; E-mail, svevans@uvic.ca.

[1]Abbreviations: LPS, lipopolysaccaharide; KDO 3-deoxy-α-D-*manno*-oct-2-ulosonic acid; CDR, complementarity determining region; SE, standard error; SPR, surface plasmon resonance; ELISA, Enzyme-linked immunosorbent assay.

 Published on Web 12/15/2009

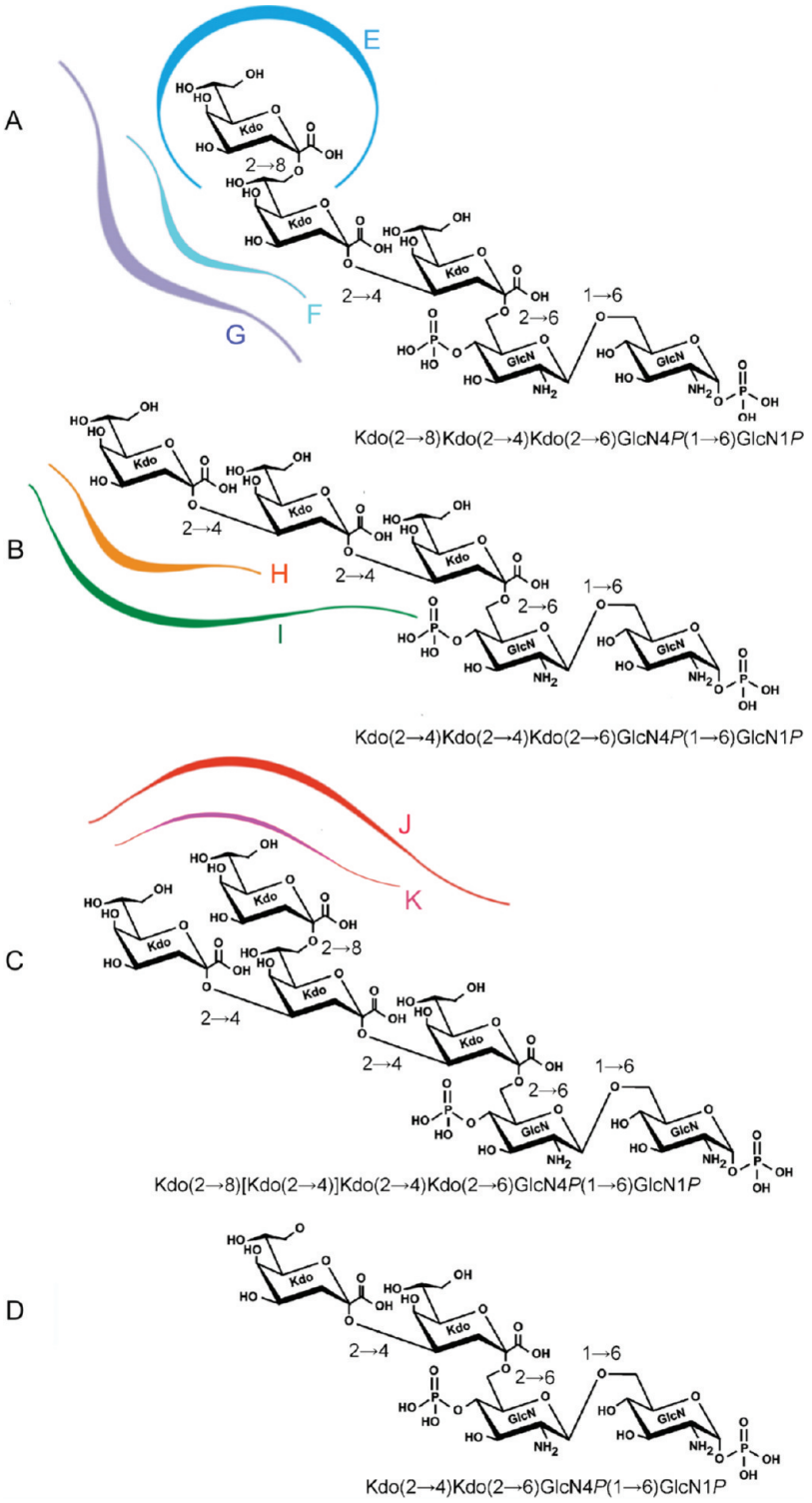

FIGURE 1: Chemical structures of oligosaccharides obtained after deacylation of chlamydial LPS. All chlamydial species investigated so far contain the pentasaccharide shown in (A) whereby the Kdo(2→8)Kdo(2→4)Kdo trisaccharide represents the Chlamydia family specific epitope. The structures shown in (B) and (C) occur in *C. psittaci* and represent species-specific epitopes. The structurally related Retype LPS of enterobacterial deep rough mutants (D) contains only a Kdo(2→4)Kdo disaccharide (*43*). Examples of epitope structures recognized by monoclonal antibodies include Kdo (E), Kdo(2→8)Kdo (F); Kdo(2→8)Kdo(2→4)Kdo (G); Kdo(2→4)Kdo (H); Kdo(2→4)Kdo(2→4)Kdo (I); Kdo(2→8)[Kdo(2→4)]Kdo(2→4)Kdo (J); Kdo(2→8)[Kdo(2→4)]Kdo (K).

have determined the structures of a number of antibodies specific for a set of similar carbohydrate antigens.

Given the increased dependency on the primary germline gene repertoires found in carbohydrate specific antibodies, they make an excellent model to study how the hereditary repertoire maintains specificity while allowing for adaptability. We initially showed that the germline codes for a binding pocket specific for bacterial monosaccharides (*9*, *11*) that utilizes a small part of the combining site for the recognition of a specific fragment of the antigen, while the rest of the combining site is free to adapt to the remainder of the antigen and provide global specificity. To further explore this observation, we selected for study two more

related monoclonal antibodies directed against carbohydrates of chlamydial LPS, characterized their binding by ELISA and surface plasmon resonance, and used X-ray diffraction techniques to determine to high resolution their structures in the presence of a number of antigens.

EXPERIMENTAL PROCEDURES

Production and Purification of Monoclonal Antibodies. BALB/c mice were immunized by a protocol described in detail by Stähli et al. (*22*). Briefly, mAb S54−10 was obtained after immunization as follows: mice (groups of 4) were injected on day 0 with Kdo(2→8)[Kdo(2→4)]Kdo(2→4)Kdo(2→6)GlcNAc4*P*-(1→6)GlcNAcol-BSA (Figure 1C) (50 μg) in PBS (125 μL) emulsified with an equal volume of Freund's complete adjuvant. One aliquot (50 μL) was injected ip, and 4 aliquots (50 μL each) were injected sc at four different sites. On day 33, again 50 μg of the antigen in PBS (50 μL) emulsified with an equal volume of Freund's incomplete adjuvant were injected ip. Seven days later, the mice were bled from the tail vein and the sera were tested for the presence of antibodies against the immunizing antigen. The mouse with the highest titer received three booster injections of 200 μg each in PBS on days 74, 75, and 76; the first one iv, the last two ip. The immunization schedule after which mAb S73−2 was obtained differed only in the booster injections, which in this case were given on days 139, 140, and 141 and the immunogen was Kdo(2→8)[Kdo(2→4)]Kdo-BSA (Figure 1K). Two days after the last injection, the animal was exsanguinated and the spleen was removed. Spleen cells were prepared and fused as described. Hybridomas were screened by ELISA using neoglycoconjugates and by immunofluorescence using cells infected with either *C. trachomatis* or *C. psittaci*. Between 4.5 and 6.5% of clones were specific for the immunizing antigen. The most relevant clones, i.e., S54−10 and S73−2, respectively, were cloned thrice by limiting dilution, isotyped with a commercially available isotype kit (Bio-Rad), and purified by affinity chromatography using an affinity support of AH-Sepharose 4B to which the ligand Kdo(2→8)-[Kdo(2→4)]Kdo(2→4)Kdo(2→6)GlcN4*P*(1→6)GlcN1*P* was conjugated by the glutardialdehyde method.

Production and Purification of Fab. Purified IgG was dialyzed into 20 mM HEPES, pH 7.5. For the preparation and purification of Fab fragments, DTT (5 mM) and EDTA (2 mM) were added to the IgG and were digested for 3 h using papain-agarose (Pierce) using an IgG to papain ratio of 1:200. The digested IgG was dialyzed overnight into 20 mM HEPES pH 7.5 and applied to a Shodex-CM 825 column equilibrated with 20 mM HEPES pH 7.5. A linear gradient of 0−0.5 M NaCl was used to elute the Fab fragments from the column.

Sequencing of Variable Regions and Germline Gene Assignment. The primary structures of both antibodies were derived from the nucleotide sequences after reverse transcription of isolated RNA and cloning after PCR amplification of cDNA. Total RNA was isolated from approximately 1×10^7 hybridoma cells using the peqGold TriFast RNA isolation kit (PeqLab Biotechnologie GmbH, Erlangen, Germany). First, strand cDNA synthesis by reverse transcription was achieved using 20 μg of isolated RNA, the oligo (dT)12−18 primer and Super-Script II reverse transcriptase (Invitrogen GmbH, Karlsruhe, Germany). For VLκ and VH mouse gene amplification the protocol and primer sets described by Barbas III et al. (*23*) were used. Amplification of VLκ of both antibodies was achieved at a reduced annealing temperature of 50 °C. For S73−2, the amplified products were then ligated by T/A cloning (TOPO-TA Cloning kit, Invitrogen) and plasmids isolated and sequenced. DNA sequencing was carried out using a *Taq* fluorescent dideoxy termination cycle sequencing kit (Applied Biosystems Inc.) and a 373 automated DNA sequencer (Applied Biosystems Inc.). For S54−10, the amplified products were first assembled into scFv by overlap extension PCR using RSC-F and RSC-B primers (*23*), digested with Sfi I (New England Biolabs, Germany), and cloned into pComb3XSS prior to sequencing (Eurofins, Germany, formerly MWG).

The putative germline gene segments from which S73−2 and S54−10 were derived were determined using the nucleotide sequence of the variable region and the IMGT/V-quest and junctional analysis (*24*).

Synthesis of Chlamydial LPS Antigens. Antigens were synthesized as previously reported (*25*−*27*).

ELISA Using Neoglycoconjugates. Neoglycoconjugates in carbonate buffer (50 mM, pH 9.2) were coated onto MaxiSorp microtiter plates (96-well, U-bottom, Nunc, Wiesbaden, Germany) at 4 °C overnight. Antigen solutions were adjusted to equimolar concentrations based on the amount of ligand present in the respective glycoconjugates in 50 μL of aliquots unless otherwise stated. Plates were washed twice in PBS supplemented with Tween 20 (0.05%, Bio-Rad) and thimerosal (0.01%, PBS-T) and subsequently blocked with PBS-T supplemented with casein (2.5%, PBS-TC) for 1 h at 37 °C on a rocker platform followed by two washings. Appropriate antibody dilutions in PBS-TC supplemented with 5% BSA (PBS−TCB) were added and incubated for 1 h at 37 °C. After two washings, peroxidase-conjugated goat antimouse IgG (heavy- and light-chain specific; Dianova, Hamburg, Germany) was added (diluted 1:1000 in PBS−TCB), and incubation was continued for 1 h at 37 °C. The plates were washed three times with PBS-T. Substrate solution was freshly prepared and composed of azino-di-3-ethylbenzthiazolinsulfonic acid (1 mg) dissolved in substrate buffer (0.1 M sodium citrate, pH 4.5), followed by the addition of hydrogen peroxide (25 μL of a 0.1% solution). After 30 min at 37 °C, the reaction was stopped by the addition of aqueous oxalic acid (2%), and the plates were read by a microplate reader (Tecan Sunrise, Crailsheim, Germany) at 405 nm.

Surface Plasmon Resonance. Kdo(2→8)Kdo(2→4)Kdo-BSA (Figure 1 epitope G) (164, 1650, and 2460 RUs), Kdo(2→4)Kdo(2→4)Kdo-BSA (Figure 1 epitope I) (280 RUs), Kdo(2→4)Kdo-BSA (Figure 1 epitope H) (980 RUs) and BSA (Sigma), as a reference protein, were immobilized on research grade CM5 sensor chips (GE Healthcare, Baie-d'Urfé, QC, Canada). Immobilizations were carried out at protein concentrations of 50 μg/mL in 10 mM acetate buffer pH 4.5 at a flow rate of 5 μL/min and using the amine coupling kit supplied by manufacturer. In all instances, analyses were carried out at 25 °C in 10 mM HEPES pH 7.4 containing 150 mM NaCl, 3 mM EDTA and 0.005% surfactant P20 at a flow rate of 40 μL/min using a BIACORE 3000 (GE Healthcare). S73−2 Fab and S54−10 monomers were separated with a Superdex 75 10/300 GL HR (GE Healthcare) column equilibrated in the running buffer mentioned above prior to analysis. Kinetic and binding constants were determined for S73−2 Fab and S54−10 Fab binding to immobilized glycoconjugates (Figure 2A,B). Rate constants were derived by data fitting to a 1:1 interaction model using BIAevaluation software version 4.1. K_Ds ± SE were derived by data fitting to a steady state affinity model using BIAevaluation software version 4.1.

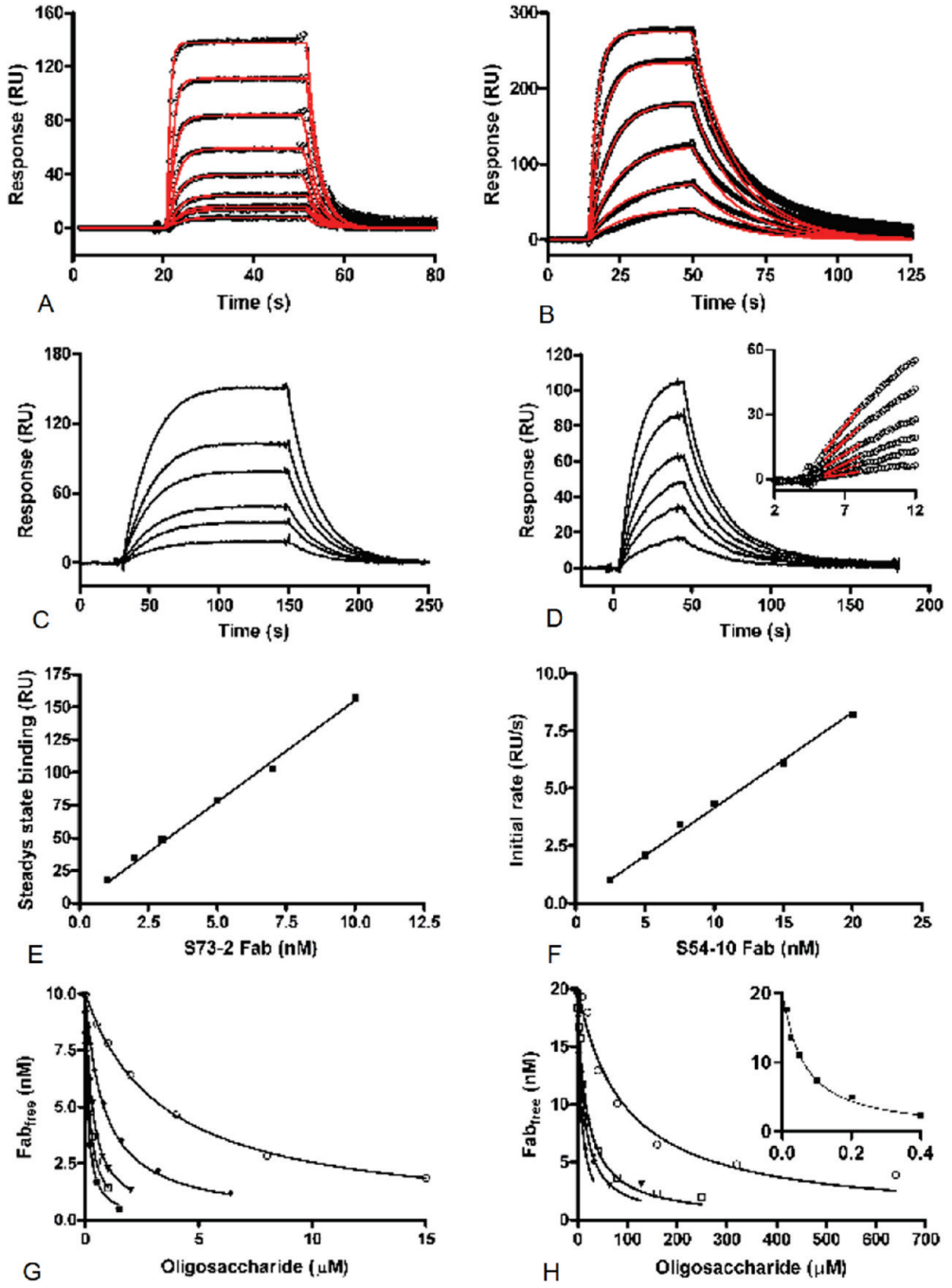

FIGURE 2: Surface plasmon resonance analysis of S73−2 and S54−10 Fab binding to different Kdo antigens. Sensorgram overlays for the binding of (A) 10, 20, 40, 80, 160, 320, 640, and 1280 nM S73−2 Fab to 160 RUs of immobilized Kdo(2→8)Kdo(2→4)Kdo-BSA and (B) 5, 10, 20, 40, 80, and 160 nM S54−10 Fab to 280 RUs of immobilized Kdo(2→4)Kdo(2→4)Kdo-BSA. The open black circles are the data points, and the red curves the fitting of the data to a 1:1 interaction model. Sensorgram overlays for the binding of (C) 1, 2, 3, 5, 7, and 10 nM S73−2 Fab to 2,460 RUs of immobilized Kdo(2→8)Kdo(2→4)Kdo-BSA and (D) 2.5, 5, 7.5, 10, 15, and 20 nM S54−10 Fab binding to immobilized Kdo(2→4)Kdo-(2→4)Kdo-BSA. Standard curves for (E) S73−2 Fab concentration assay based on the steady state binding data from C and (F) S54−10 Fab concentration assay based on initial mass transport limited rates from the sensorgrams in (D): inset shows linear fitting (red lines) of the initial data points (open black circles). Fitting to a solution affinity model of data for the inhibition of (G) S73−2 Fab binding to 1650 or 2460 RUs of immobilized Kdo(2→8)Kdo(2→4)Kdo-BSA and (H) S54−10 Fab binding to 280 RUs of immobilized Kdo(2→4)Kdo(2→4)Kdo-BSA by various saccharides (○) Kdo; (♦)Kdo(2→8)Kdo; (▼)Kdo(2→4)Kdo; (□)Kdo(2→8)Kdo(2→4)Kdo; (■)Kdo(2→4)Kdo(2→4)Kdo.

Previously described SPR solution affinity methods were used (*9*, *28*) to determine the affinity of the Fab fragments for free Kdo oligosaccharides. Solution affinity analysis was carried out on both antibodies. The glycoconjugate Kdo(2→8)Kdo-(2→4)Kdo-BSA (Figure 1 epitope G) was immobilized and used for determination of solution affinities for S73−2, while Kdo-(2→4)Kdo(2→4)Kdo-BSA glycoconjugate (Figure 1 epitope I) was used for S54−10 (Figure 2). Concentration assay standard curves for S73−2 Fab binding to Kdo(2→8)Kdo(2→4)Kdo-BSA and S54−10 Fab binding to Kdo(2→4)Kdo(2→4)Kdo-BSA were collected in concentration ranges of 1−10 and 2.5−20 nM, respectively. The S73−2 standard curve was based on steady state data collected at Fab concentrations that were much lower than the K_D (300 nM); at these Fab concentrations the steady state binding response is directly proportional to Fab concentration (Figure 2C, 2E). The S54−10 standard curve was based on

Table 1: Data Collection and Refinement Statistics of S73-2 and S54-10

	S73−2				S54−10
parameter	Kdo	Kdo(2→4)Kdo	Kdo(2→4)Kdo (2→4)Kdo	Kdo(2→8)Kdo (2→4)Kdo	Kdo(2→4)Kdo (2→4)Kdo
cell constants *a*, *b*, *c* (Å)	46.00, 81.80, 127.98	46.34, 80.94, 128.10	45.94, 81.97, 128.24	47.05, 80.80, 128.75	64.98, 53.36, 142.26
Z	1	1	1	1	2
space group	$P2_12_12_1$	$P2_12_12_1$	$P2_12_12_1$	$P2_12_12_1$	$P2_1$
observations	196783	121070	123465	180729	106610
unique reflections	44182	25575	28056	38610	28890
resolution[a]	19.86−1.80 (1.86−1.80)	19.86−2.15 (2.23−2.15)	19.80−2.10 (2.17−2.10)	19.99−1.90 (1.97−1.90)	19.98−2.60 (2.69−2.60)
completeness (%)	96.9 (93.4)	94.9 (92.2)	96.6 (98.6)	97.8 (99.11)	97.3 (95.8)
R_{sym} (%)[b]	4.9 (33.6)	6.1 (29.6)	9.4 (22.0)	7.2 (35.3)	9.7 (32.5)
$I/\sigma(I)$	14.4 (3.8)	11.6 (3.8)	8.7 (4.8)	11.1 (3.8)	8.0 (3.2)
number of atoms	3704	3590	3727	3773	6851
polypeptide	341	3391	3349	3377	6497
sugar	15	33	48	48	96
solvent	278	166	330	348	258
R_{work}[c]	20.71	21.43	21.58	21.17	21.33
R_{free}	24.86	26.01	26.05	24.90	26.46
B factor (Å^2)					
protein	27.52	34.0	31.53	26.95	35.45
ligand	25.42	35.75	37.97	26.85	40.71
water	31.56	34.35	38.75	31.63	32.84
deviations from ideal geometry (rms)					
bonds	0.011	0.006	0.006	0.004	0.004
angles	1.374	1.065	0.944	0.942	0.890
dihedrals	17.482	18.01	16.866	16.270	18.012
Ramachandran plot (%)					
most favored	88.9	88.5	89.1	90.7	88
allowed	10.6	11	10.6	9.1	12
disallowed	0.6	0.6	0.3	0.3	1
PDB Code	3HZM	3HZK	3HZY	3HZV	3I02

[a]Value in parentheses are for high resolution shell. [b]$R_{sym} = \sum\sum_i|I_i - \langle I\rangle|/\sum\langle I\rangle$, where I is the integrated intensity of a reflection. [c]$R_{work} = \sum_{hkl}||F_o| - k|F_c||/\sum_{hkl}|F_o|$.

mass transport limited data wherein the initial binding rates are directly proportional to Fab concentration (Figure 2D,F). For each antibody, several concentrations of different oligosaccharides were pre-equilibrated with fixed concentrations of Fab, 10 nM for S73−2 and 20 nM for S54−10, prior to injection over glycoconjugate surfaces for determination of free Fab concentrations at different oligosaccharide concentrations. The concentrations of oligosaccharide were plotted against free Fab concentrations and the dissociation constants ± SE were calculated by fitting the data to a solution affinity model using BIAevaluation software version 4.1 (Figures 2G,H).

Crystallization of Liganded S73−2 and S54−10. Purified Fab fragments of S54−10 and S73−2 were buffer exchanged into 20 mM HEPES pH 7.5 and concentrated to 15 mg/mL. The Fab fragments were mixed with 50 mM Kdo and were screened using Hampton crystal screens I and II, as well as custom screens. Optimal crystals of S73−2 Fab grew to a large size (1 mM^3), and the optimal conditions were in 50 mM Tris pH 8.0, 35 mM $MgCl_2$, 25 mM $ZnCl_2$, 10% PEG 4000, and 10% ethylene glycol. Excellent crystals of S73−2 in complex with other Kdo ligands appeared in identical conditions. Crystals of S54−10 grew under similar conditions to S73−2, with excellent crystals growing in 10% PEG 4000 and 50 mM sodium cacodylate pH 6.5.

Data Collection, Structure Determination, and Refinement. Crystals were flash frozen to −160 °C using an Oxford Cryostream 700 crystal cooler (Oxford Cryosystems). Data were collected with a Rigaku R-AXIS IV++ area detector (Rigaku, Japan) coupled to a MM-002 X-ray generator with Osmic "blue" optics (Osmic, College Station, TX) and processed using Crystal Clear/d*trek (Rigaku). The structure of the liganded S73−2 and S54−10 Fab was solved by molecular replacement using PHASER (*29*) as implemented in CCP4 (*30*) using the previously solved liganded S25−2 structure (PDB accession code 1Q9R). SetoRibbon (Evans, unpublished) and Coot (*31*) were used for manual fitting of σ_A-weighted $2F_o - F_c$ and $F_o - F_c$ electron density maps. Restrained refinement allowing isotropic thermal motion was carried out with REFMAC5 and *phenix.refine* as implemented in CCP4 and Phenix (*30*, *32*). The final refinement and model statistics are given in Table 1.

RESULTS

Specificity of S73−2 and S54−10 by ELISA. In an effort to generate antibodies specific for the LPS structure of *C. psittaci*, BALB/c mice were immunized with Kdo(2→8)[Kdo(2→4)]-Kdo(2→4)Kdo(2→6)GlcNAc(1→6)GlcNAcol-BSA (Figure 1C) glycoconjugate or with Kdo(2→8)-[Kdo(2→4)]Kdo-BSA glycoconjugate (Figure 1C, epitope J), yielding mAb S54−10 (IgG1κ) and S73−2 (IgG1κ), respectively. The specificity and relative affinities of the antibodies were assessed by ELISA using a variety of glycoconjugates representing the complete carbohydrate backbone of chlamydial LPS (Figure 1A−D) and partial structures thereof (Figure 1 epitopes E−K; Table 2). The antibody S73−2 displayed a broad specificity, binding with the same affinity to its immunizing antigen Kdo(2→8)[Kdo(2→4)]Kdo (Figure 1, epitope K) and all structures containing the (2→4)-(2→4)-linked trisaccharide (Figure 1, epitope G; Table 2) or the branched Kdo

Table 2: Affinity of S73-2 and S54-10 IgG to Various Chlamydial LPS Fragments as Determined by ELISA

ligand conjugated to BSA[a]	epitope structure[a]	S73−2 mAb conc (ng/mL) yielding OD_{405} >0.2 in ELISA using 2 pmol/cup	S73−2 mAb conc (ng/mL) yielding OD_{405} >0.2 in ELISA using 20 pmol/cup	S54−10 mAb conc (ng/mL) yielding OD_{405} >0.2 in ELISA using 2 pmol/cup	S54−10 mAb conc (ng/mL) yielding OD_{405} >0.2 in ELISA using 20 pmol/cup
Kdo	E	250	63	250	125
Kdo(2→8)Kdo	F	250	63	250	63
Kdo(2→8)Kdo(2→4)Kdo	G	16	4	250	63
Kdo(2→8)Kdo(2→4)Kdo(2→6)GlcNAc4*P*(1→6)GlcNAcol	A	32	8	500	125
Kdo(2→4)Kdo	H	8	4	63	8
Kdo(2→4)Kdo(2→6)GlcN4*P*(1→6)GlcN1*P*	C	500	63	1000	500
Kdo(2→4)Kdo(2→4)Kdo	I	4	4	4	4
Kdo(2→4)Kdo(2→4)Kdo(2→6)GlcNAc4*P*(1→6)GlcNAcol	B	8	4	8	8
Kdo(2→8)[Kdo(2→4)]Kdo(2→4)Kdo	J	4	4	4	4
Kdo(2→8)[Kdo(2→4)]Kdo(2→4)Kdo(2→6)GlcN4*P* (1→6)GlcN1*P*	D	4	4	4	4
Kdo(2→8)[Kdo(2→4)]Kdo	K	4	4	16	16

[a]Refers to epitope structures in Figure 1.

tetrasaccharide (Figure 1B, epitope I; 1C, epitopes J, K; Table 2). The antibody cross-reacted with the family specific Kdo-(2→8)Kdo(2→4)Kdo linked trisaccharide (Figure 1, epitope G) and with both the (2→4) and (2→8)-linked disaccharides (Figure 1, epitopes F, H), indicating that the antibody may not discriminate between *C. psittaci* and the other chlamydiae species (Table 2). Examination of the ELISA data against the Kdo disaccharides showed that the antibody preferentially bound to the (2→4) linkage (Figure 1B, epitope H) and would bind to any epitope presented that contained this linkage. When the Kdo antigens were linked to the lipid A backbone of native LPS (1,4′-biphosphorylated β1.6-linked GlcNAc disaccharide) (Figure 1A−D), S73−2 showed preferential binding to the branched tetrasaccharide (Figure 1C, epitope J) and the linear Kdo(2→4)Kdo-(2→4)Kdo trisaccharide (Figure 1B, epitope I).

MAb S54−10 bound to the *C. psittaci*-specific structures to an extent similar to S73−2 but exhibited lower affinity for all other antigens tested. Like S73−2, S54−10 did not differentiate between antigens containing the branched Kdo tetrasaccharide or the (2→4)-(2→4)-linked trisaccharide but did bind to the (2→8)-(2→4)-linked trisaccharide with weaker affinity than S73−2.

Affinities of S73−2 and S54−10 for Kdo Oligosaccharides. The affinities of Fabs from S73−2 and S54−10 toward carbohydrate antigens containing Kdo were also examined by surface plasmon resonance (SPR). Kinetic and binding constants for S73−2 Fab and S54−10 Fab were determined with immobilized glycoconjugates (Figure 2A,B and Table 3) and by solution affinity to free oligosaccharides (Figure 2C−H, Table 4). The K_Ds as determined by Fab binding to immobilized glycoconjugate were in good agreement with those determined by solution affinity analyses with the corresponding oligosaccharides. The low estimated standard errors show that the data obtained were an excellent fit to the binding model; however, the inherent difficulties in accurately measuring the concentrations of the proteins and especially the small quantities of antigen used means that true standard error for on-rates and K_Ds are probably of the order of ±25%. The SPR data were consistent with the ELISA data and confirmed that S73−2 bound with higher affinity to (2→4) linkage containing oligosaccharides and that S73−2 bound equally well to either the (2→8)-(2→4)- or the (2→4)-(2→4)-linked trisaccharide

Table 3: Kinetic and Binding Constants of S73-2 and S54-10 for Immobilized Glycoconjugates Determined by SPR

antibody	immobilized glycoconjugate[a]	ka ($\times 10^6$ 1/ms)	kd (1/s)	K_D ($\times 10^{-7}$ M) ± SE
S54−10	Kdo(2→4)-Kdo(2→4)Kdo[b]	2	0.07	0.3 ± 0.01
S73−2	Kdo(2→8)-Kdo(2→4)Kdo[c]	1	0.4	3 ± 0.3
S73−2	Kdo(2→4)Kdo[d]	N/A[e]	N/A	2 ± 0.2

[a]BSA glycoconjugates. [b]Collected on a conjugate surface density of 280 RUs. [c]Collected on a conjugate surface density of 164 RUs. [d]Collected on a conjugate surface density of 980RUs. [e]Dissociation rate too fast for kinetic analysis.

Table 4: Solution Affinities of S73-2 and S54-10 Fab for Free Kdo Ligands Determined by SPR

antigen	K_D ($\times 10^{-7}$ M) ± SE S54−10[a]	K_D ($\times 10^{-7}$ M) ± SE S73−2[b]
Kdo	900 ± 100	30 ± 0.6
Kdo(2→4)Kdo	90 ± 8	3 ± 0.1
Kdo(2→8)Kdo	60 ± 6	8 ± 0.4
Kdo(2→4)Kdo(2→4)Kdo	0.5 ± 0.03	1 ± 0.05
Kdo(2→8)Kdo(2→4)Kdo	200 ± 10	2 ± 0.03

[a]Data collected using Kdo(2→4)Kdo(2→4)Kdo-BSA surface density of 280 RU. [b]Data collected using Kdo(2→8)Kdo(2→4)Kdo-BSA surface density of 1700 and 2400 RU.

(Figure 1, epitopes G, I; Tables 3,4). Unlike S73−2, S54−10 bound with very high affinity to Kdo(2→4)Kdo(2→4) and bound only weakly to the Kdo(2→8)Kdo(2→4) trisaccharide (Tables 3,4). Thus S73−2 is a multispecific antibody capable of recognizing the two trisaccharide structures with equal affinity, while S54−10 is highly specific for the Kdo(2→4)Kdo(2→4) trisaccharide.

Germline Genes in Chlamydia-Specific Antibodies. The sequences of four chlamydial LPS specific antibodies, S25−2, S45−18, S73−2, and S54−10 are homologous in sequence, having derived from the same set of germline V-gene segments

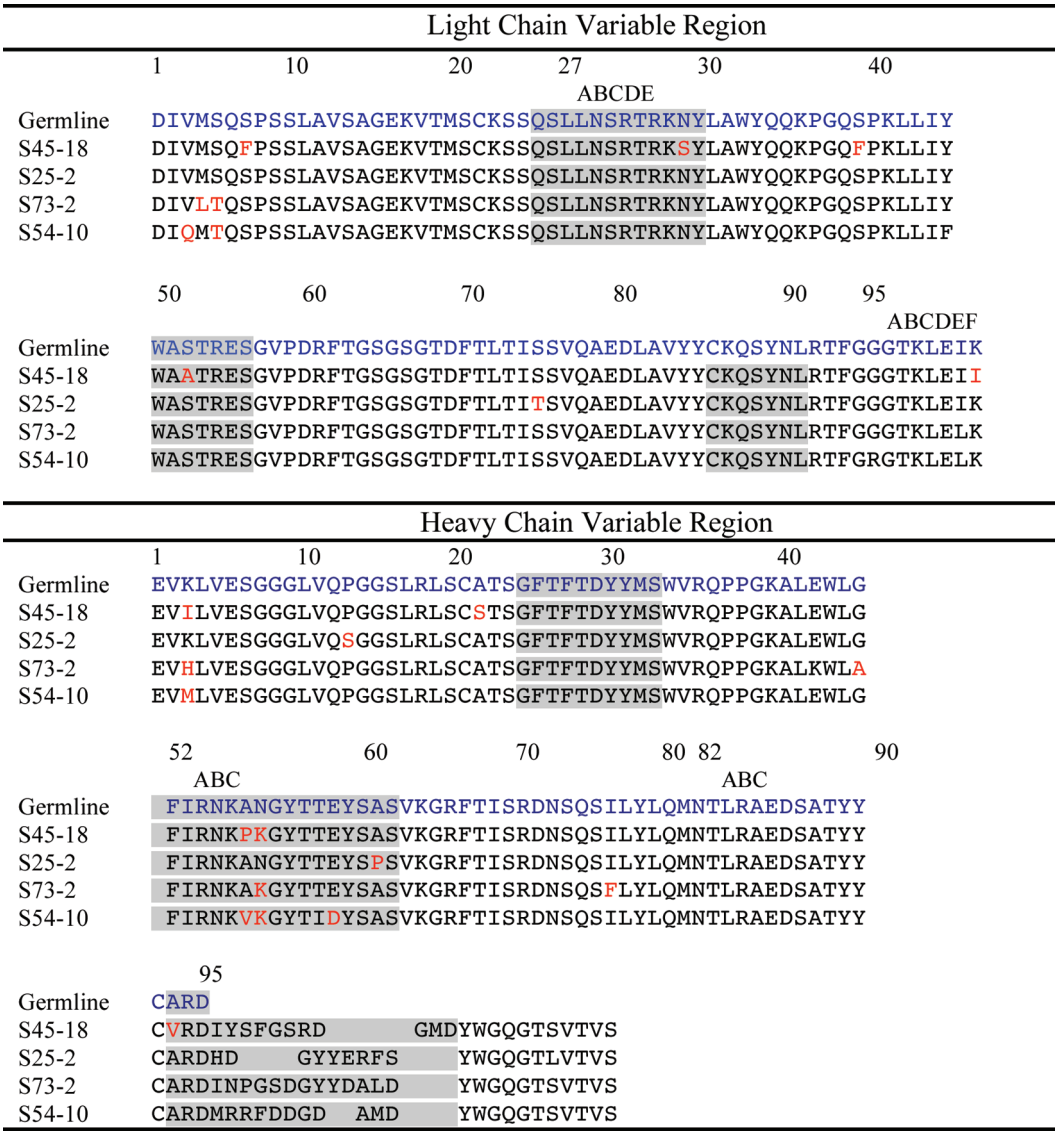

FIGURE 3: Variable region sequences of antibodies S45−18, S25−2, S73−2, S54−10, and putative germline gene sequence. Residues which differ from the germline sequence are shown in red. Putative germline gene segments were determined using IMGT/V-Quest (*24*). Residues are numbered according to Kabat (*44*) as implemented in AbNum (*45*)

(Figure 3 and Table 5). The variable light chain region of all four antibodies is derived from the same germline gene IgGκV8−21, while the V region of the heavy chain for all four antibodies is derived from the gene IgHV7−3. The antibodies differ in their germline gene usage from the genes IgGκJ (light chain) and the J and D genes in the heavy chain (Table 5). The use of different J and D genes in the heavy chain segments is responsible for the generation of divergent CDR H3 sequences, which is the primary source of sequence variation among these antibodies.

The antibodies also differ in their degree of affinity maturation. With the V-region derived from the germline genes IgHV7−3 and IgGκV8−21, S45−18 has a total of nine mutations away from germline, S73−2 and S54−10 have six mutations, and S25−2 has the fewest with only three mutations (Figure 3). Most of these mutations have occurred within the framework region, although all four antibodies have mutations in CDR H2.

Structures of Liganded S73−2 and S54−10. The Fab fragment of S73−2 was cocrystallized with Kdo, Kdo(2→4)Kdo, Kdo(2→4)Kdo(2→4)Kdo, and Kdo(2→8)Kdo(2→4)Kdo (Figure 1, epitopes E, H, I, G), all of which exhibit excellent electron density in the combining site (Figure 4). S54−10 was cocrystallized with

Table 5: Germline Gene Segment Usage of the Variable Regions of Anti-Chlamydial LPS Antibodies

	S45−18	S25−2	S73−2	S54−10
		Light Chain (κ)		
V-gene	IGKV8−21*01	IGKV8−21*01	IGKV8−21*01	IGKV8−21*01
J-gene	IGKJ2*02	IGKJ2*02	IGKJ1*01 or IGKJ5*01	IGKJ1*01
		Heavy Chain		
V-gene	IGHV7−3*02	IGHV7−3*02	IGHV7−3*02	IGHV7−3*02
D-gene	IGHD1−1*01	IGHD2−9*01	IGHD2−3*01	IGHD2−14*01
J-gene	IGHJ4*01	IGHJ3*01	IGHJ4*01	IGHJ4*01

the (2→4)-(2→4)-linked Kdo trisaccharide (Figure 1, epitope I), which also displayed unambiguous electron density (Figure 4). S73−2 contained a single molecule per asymmetric unit, while S54−10 contained two molecules per asymmetric unit (Table 1). The two molecules in the asymmetric unit of S54−10 are nearly identical in structure and overlap with an rmsd of 0.5 Å over all

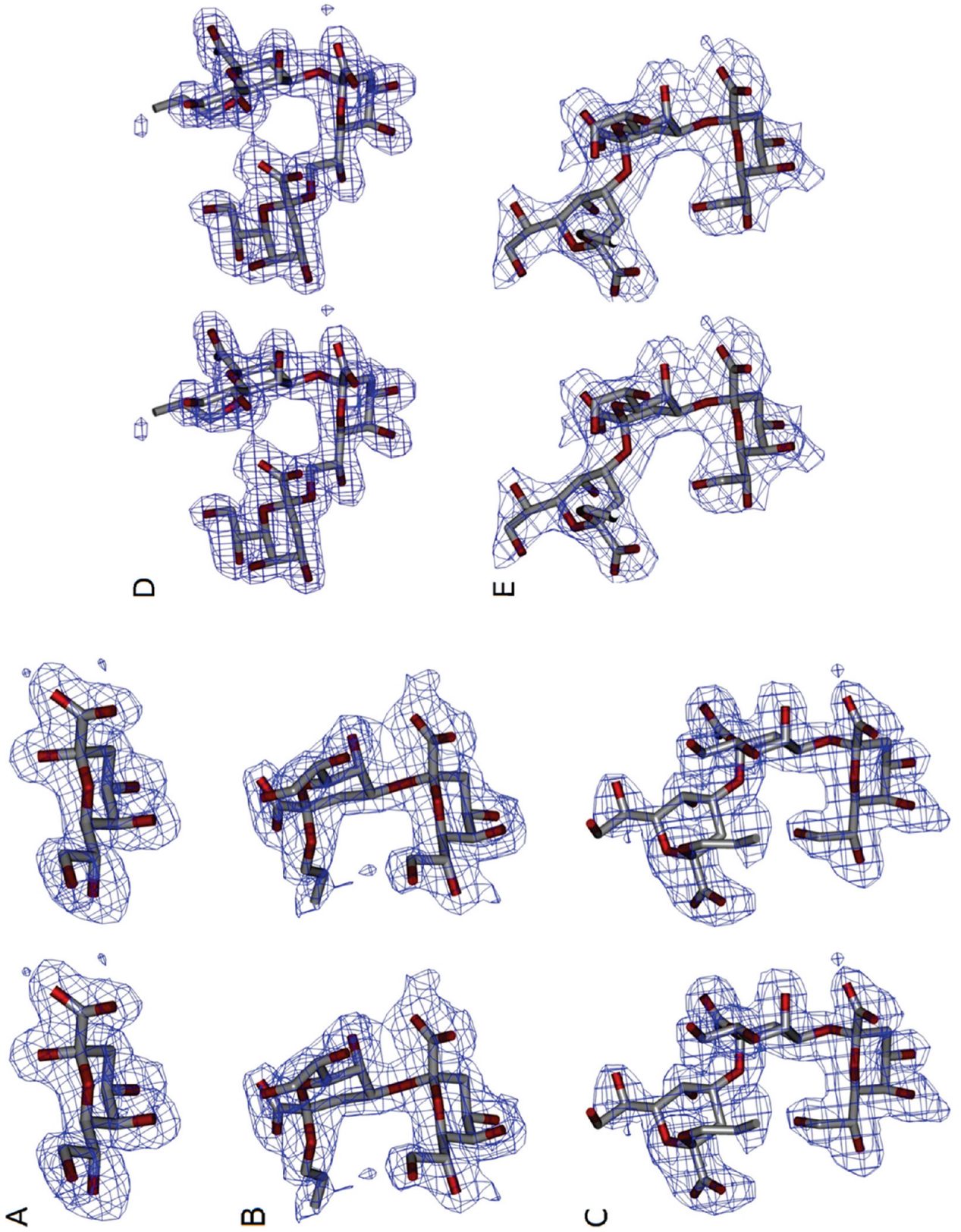

FIGURE 4: Observed $2F_0 - F_c$ σ_A-weighted electron density maps of antigens bound to Fab, contoured to 1.0σ. (A) S73−2 with Kdo; (B) S73−2 with Kdo(2→4)Kdo; (C); S73−2 with Kdo(2→4)Kdo-(2→4)Kdo; (D) S37−2 with Kdo(2→8)Kdo(2→4)Kdo; (E) S54−10 with Kdo(2→4)Kdo(2→4)Kdo.

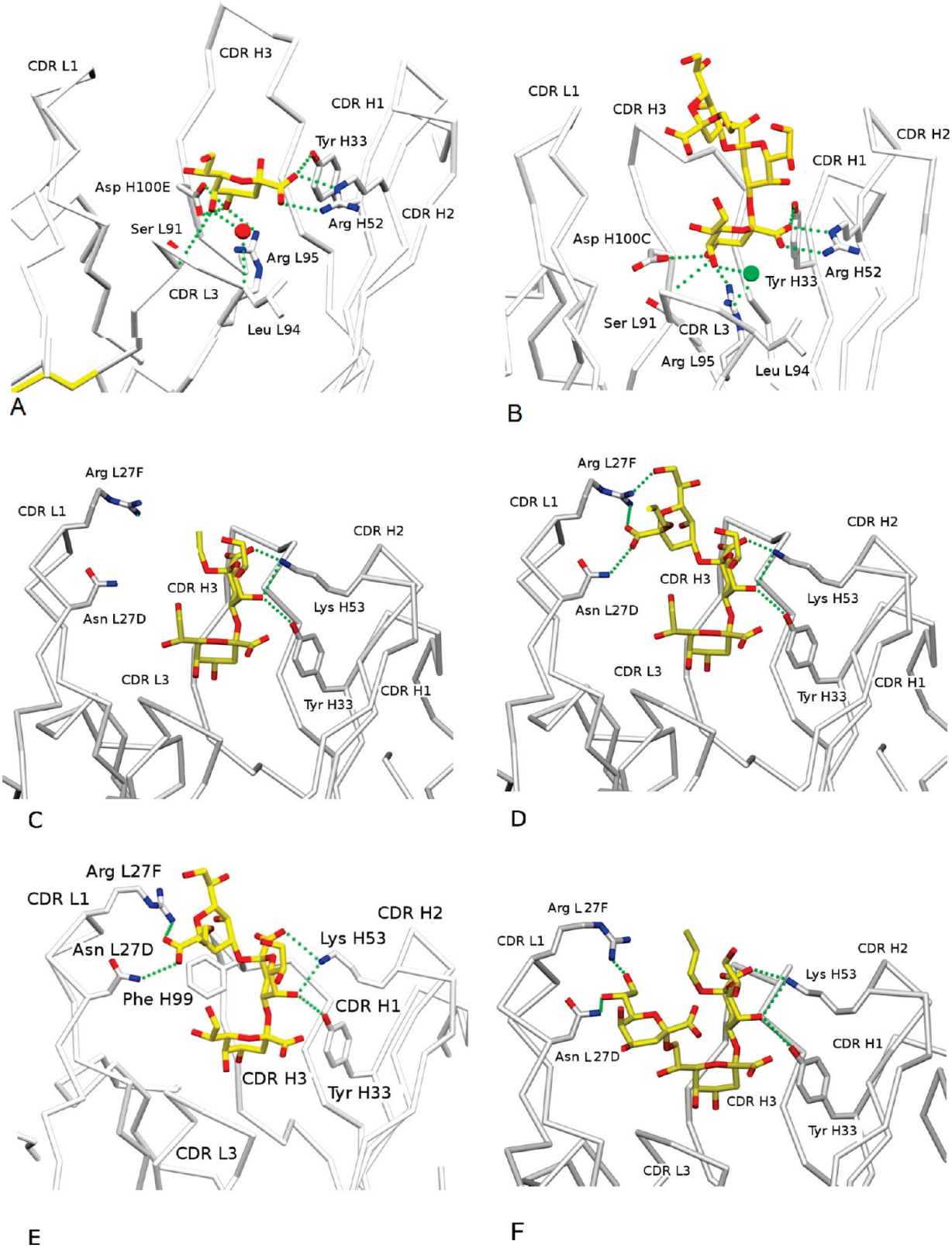

FIGURE 5: Antibody combining site binding interactions of (A) S73−2 with Kdo; (B) S54−10 with terminal Kdo residue in Kdo(2→4)Kdo-(2→4)Kdo; (C) S73−2 with Kdo(2→4)Kdo; (D); S73−2 with Kdo(2→4)Kdo(2→4)Kdo; (E) S54−10 with Kdo(2→4)Kdo(2→4)Kdo; (F) S73−2 with Kdo(2→8)Kdo(2→4)Kdo.

α-carbon atoms. The two molecules display the same main chain and side chain conformations throughout the variable region but exhibit slight differences in the constant region apparently owing to crystal packing. Both S73−2 and S54−10 showed good stereochemistry and exhibited well-ordered main chain and side chain electron density throughout all of the variable regions and all but a few residues of the constant regions.

The terminal Kdo residue in both structures bound within a solvent-excluded pocket, using an identical array of hydrogen bonds and charged interactions (Figure 5A,B). The Kdo binding

pocket is formed by residues on CDR L3, the base of CDR H3, and residues from CDR H1 and H2. The carboxyl group on the Kdo forms a salt bridge to ArgH52 as well as a hydrogen bond to TyrH33. The Kdo hydroxyl groups at positions 4 and 5 form hydrogen bonds to AspH100E, ArgL95, and SerL91 (Figure 5A). S73−2 forms two additional interactions outside of the binding pocket to Kdo(2→4)Kdo, with a salt bridge between the carboxyl on the second Kdo residue and LysH53 (Figure 5C). The O5 of the second Kdo also forms interactions in the combining site of S73−2 with hydrogen bonds to LysH52 and TyrH33 (Figure 5C). The interactions of S73−2 with Kdo(2→4)Kdo(2→4)Kdo are similar to those of the Kdo(2→4)Kdo disaccharide, except interactions are formed with the third Kdo residue to ArgL27F and AsnL27D (Figure 5D). S54−10 in complex with Kdo-(2→4)Kdo(2→4)Kdo makes interactions with the same ligand similar to those on S73−2, except a stacking interaction is formed with PheH99 on CDR H3 (Figure 5E). The ligand Kdo-(2→8)Kdo(2→4)Kdo forms interactions with LysH53, TyrH33, ArgL27F, and AsnL27D (Figure 5F), and rather than recognize a terminal Kdo in the binding pocket, the middle Kdo of the trisaccharide is bound (Figure 5F).

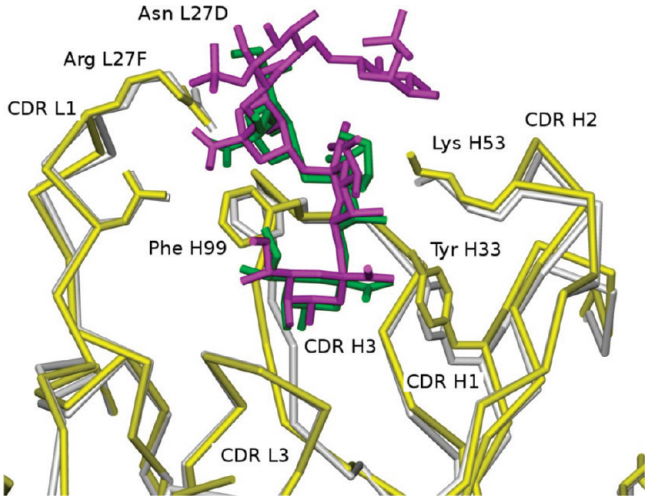

FIGURE 6: Least squares overlap of α-carbon atoms of S45−18 (yellow) in complex with Kdo(2→4)Kdo(2→4)Kdo(2→6)GlcN4P-(1→6)GlcN1P (magenta) and S54−10 (white) in complex with Kdo-(2→4)Kdo(2→4)Kdo (green) reveals convergent binding modes despite differing CDR H3 sequences. Overlap was performed in *Phenix* (*31*).

DISCUSSION

Conserved Germline Gene Usage and Inherited Immunity. The humoral immune system is capable of recognizing an enormous array of potential antigens, and this diversity in the antibody response is largely coded for by genetic recombination of V-, D-, and J-gene segments (*12*). This genetic recombinatorial event is estimated to be capable of generating as many as 1.2×10^7 possible antibodies in mice (*33*). Remarkably, despite this enormous potential diversity, these four antibodies that were raised against distinct Kdo oligosaccharides all make use of a similar set of V and J genes in the light chain, and the same set of V genes in the heavy chain (Table 5). This redundant germline gene usage suggests that the recognition of Kdo is evolutionarily conserved, and that even in a naïve organism there exist B-cells expressing appropriate combinations of these particular V-gene segments for the surveillance of Kdo monosaccharide residues.

Such observed germline gene restriction is not unique to chlamydial carbohydrate antigens and has been observed in the antibody response to several other T-cell independent antigens, including the capsular polysaccharides from *Haemophilus influenzae* in both mice and humans (*34*, *35*), *Streptococcus pneumoniae* (*36*), *Cryptococcus neoformans*, (*37*, *38*) and *Neisseria meningitidis* (*39*). This evidence of an inherited immune response is of particular importance for T-cell independent antigens, which have an increased dependency on the primary germline gene response. The immune response to carbohydrates of chlamydial LPS (*3*−*11*) is an example of how the immune system has evolved to code for antibody gene segments that serve to recognize conserved monosaccharide residues from pathogenic bacteria.

Differing CDR H3 Sequences Result in Convergent Binding Modes. Several studies implicate CDR H3 as mainly responsible for dictating antibody specificity (e.g., refs (*40*, *41*)), and it has been shown that changes in CDR H3 sequence and length are sufficient to alter specificity (*42*). Antibody S45−18 (*11*) differs from S54−10 in sequence but not length of CDR H3, yet exhibits preferential binding to the same ligand, i.e., Kdo(2→4)Kdo(2→4) (Table 2; Figure 3; Figure 1, epitope I). Examination of the superimposed combining sites of S45−18 and S54−10 together with the Kdo(2→4)Kdo(2→4)Kdo ligand shows that the two antibodies utilize a convergent binding mode (Figure 6). Both antibodies form the conserved set of interactions between the specificity pocket and the terminal Kdo residue first reported for S25−2 (*9*, *11*), and LysH53 on CDR H2 of both antibodies forms a salt bridge to the carboxyl group and a hydrogen bond to O5 of the second Kdo residue (Figure 6). Remarkably, the two antibodies form similar interactions with PheH99 in CDR H3 despite the markedly different sequences arising from two unrelated D- and J-gene segments, illustrating that the function of CDR H3 is not just to provide specific interactions with the ligand but also to provide a specific architecture in the combining site. The differing D, J gene usage resulting in identical CDR H3 interactions also demonstrates a clear redundancy in the ability of multiple D, J gene arrangements to generate identical binding modes.

Differential Recognition of Kdo(2→4) Kdo(2→4)Kdo by S73−2. The antibody S73−2 has a fairly broad specificity, as it is equally capable of recognizing the Kdo(2→4)Kdo(2→4)Kdo and the Kdo(2→8)Kdo(2→4)Kdo epitopes (Figure 2; Tables 2−4; Figure 1, epitopes I, G). This is in contrast to S25−2, which also displays significant promiscuity in antigen binding but binds the Kdo(2→4)Kdo(2→4)Kdo epitope only weakly (*9*, *11*). Although S73−2 maintains an affinity for the antigen comparable to S45−18 (*11*) and S54−10, the mode of recognition differs fundamentally. While S73−2 binds the terminal (first) Kdo residue through the binding pocket with additional interactions from CDRs H2 and L1 to the second Kdo residue (Figure 5D), S54−10 and S45−18 both form hydrophobic stacking interactions between PheH99 of CDR H3 and the third Kdo residue. The observed promiscuity of S73−2 may partly be due to the absence of this stacking interaction as much as the observed specificity of S54−10 and S45−18 can be partly attributed to its presence; however, the complete absence of interactions through CDR H3 between S73−2 and the antigen defies the convention whereby antibody specificity is primarily conferred by H3 (*40*−*42*).

Further insight is gained by a comparison of S73−2 with S25−2, the latter which binds Kdo(2→4)Kdo(2→4)Kdo only weakly and cannot form stacking interactions to the antigen through CDR H3 (*9*, *11*). These structures show that the difference

in affinity can be traced to a single amino acid in CDR H2. In the case of S73−2, S54−10, and S45−18, LysH53 forms a salt bridge to the carboxyl of the second Kdo residue while S25−2 maintains the germline Asp that can form only a simple and more geometrically strained hydrogen bond (Figure 3). Thus, it appears that the specificity of S73−2 for the Kdo(2→4)Kdo-(2→4)Kdo trisaccharide is mediated primarily through a single specific interaction via CDR H2, rather than CDR H3, which again indicates that the specificity of this antibody is an exception to the rule that CDR H3 primarily drives the antibody specificity (*42*).

Recognition of an Internal Kdo Residue by S73−2. The homologous antibodies S25−2, S54−10, and S45−18 all recognize a Kdo trisaccharide by binding the terminal Kdo residue of these respective antigens by an evolutionarily conserved specificity pocket, leaving the remaining moieties of the ligand to bind to an open groove on the surface of the combining site (*9*, *11*). In contrast, the specificity pocket of S73−2 binds to the Kdo-(2→8)Kdo(2→4)Kdo trisaccharide antigen through an internal Kdo residue (Figure 5F). This rather unique binding arises from the formation of a salt bridge between LysH53 on CDR H2 and the central Kdo residue.

This illustrates the adaptability of this antibody and lends credence to the idea that the germline can code for antibodies that are specific for bacterial monosaccharides yet remain promiscuous over a range of related oligosaccharide antigens and that fine specificity is largely dictated by differences in CDR H3 and through affinity maturation. S73−2 makes no interactions with its ligands via CDR H3 because the polypeptide loop is longer and projects away from the combining site (Figure 5A), which contributes to that antibody's increased adaptability.

CONCLUSIONS

A striking feature of these four antibodies raised against Chlamydial Kdo antigens is the use of a limited number of conserved germline gene segments to form highly adaptable antibodies capable of recognizing families of immunologically distinct antigens. The recognition of the Kdo(2→4)Kdo-(2→4)Kdo trisaccharide by S45−18 and S54−10 illustrates an interesting redundancy in germline gene segments in that different D- and J-gene segments can be recombined to yield antibodies that display convergent binding modes of a specific antigen. Such redundancy pathways directed toward important antigens would confer a clear survival advantage by maximizing the chances of obtaining a successful B-cell mediated antibody response to the pathogen.

The diversity in antigen recognition by a limited set of germline gene segments is well illustrated by a comparison of the structures of these four homologous antibodies, where modest changes in sequence result in a diverse range of specific or promiscuous antibodies. S73−2 recognizes multiple epitopes with equal affinity, due in part to a long and flexible CDR H3 sequence that makes no direct contact with the ligands, while the structure of CDR H3 in S54−10 and S45−18 confers a higher degree of specificity. Finally, comparison of the structures of S73−2 and S25−2 demonstrates that CDR H3 alone is not sufficient for dictating the specificity of these antibodies as it can also be modulated by a single amino acid substitution in CDR H2.

ACKNOWLEDGMENT

The technical assistance of Nadine Harmel, Veronika Susott, Ute Agge, and Irina von Cube is appreciated.

REFERENCES

1. Bowie, W. R., Caldwell, H. D., Jones, R. P., Mardh, P.-A., Ridgway, G. I., Schachter, J (Eds.), (1990) Chlamydial Infections, Cambridge University Press, Cambridge, U.K.
2. Rund, S., Lindner, B., Brade, H., and Holst, O. (2000) Structural analysis of the lipopolysaccharide from *Chlamydophila psittaci* strain 6BC. *Eur. J. Biochem. 267*, 5717–5726.
3. Müller-Loennies, S., Gronow, S., Brade, L., MacKenzie, C. R., Kosma, P., and Brade, H. (2006) A monoclonal antibody against a carbohydrate epitope in lipopolysaccharide differentiates *Chlamydophila psittaci* from *Chlamydophila pecorum, Chlamydophila pneumoniae* and *Chlamydia trachomatis*. *Glycobiology 16*, 184–196.
4. Fu, Y., Baumann, M., Kosma, P., Brade, L., and Brade, H. (1992) A synthetic glycoconjugate representing the genus-specific epitope of chlamydial lipopolysaccharide exhibits the same specificity as its natural counterpart. *Infect. Immun. 60*, 1314–1321.
5. Peterson, E. M., De La Maza, L. M., Brade, L., and Brade, H. (1998) Characterization of a neutralizing monoclonal antibody directed at the lipopolysaccharide of *Chlamydia pneumoniae*. *Infect. Immun. 66*, 3848–3855.
6. Müller-Loennies, S., MacKenzie, C. R., Patenaude, S. I., Evans, S. V., Kosma, P., Brade, H., Brade, L., and Narang, S. (2000) Characterization of high affinity monoclonal antibodies specific for chlamydial lipopolysaccharide. *Glycobiology 10*, 121–130.
7. Brade, L., Rozalski, A., Kosma, P., and Brade, H. (2000) A monoclonal antibody against 3-deoxy-α-D-*manno*-oct-2-ulosonic acid (Kdo) trisaccharide αKdo(2→4)αKdo(2→4)αKdo of *Chlamydophila psittaci* 6BC lipopolysaccharide. *J. Endotoxin Res. 6*, 361–368.
8. Brade, L., Gronow, S., Wimmer, N., Kosma, P., and Brade, H. (2002) Monoclonal antibodies against 3-deoxy-α-D-*manno*-oct-2-ulosonic acid (Kdo) and D-*glycero*-α-D-*talo*-oct-2-ulosonic acid (Ko). *J. Endotoxin Res. 8*, 357–364.
9. Brooks, C. L., Müller-Loennies, S., Brade, L., Kosma, P., Hirama, T., MacKenzie, C. R., Brade, H., and Evans, S. V. (2008) Exploration of specificity in germline monoclonal antibody recognition of a range of natural and synthetic epitopes. *J. Mol. Biol. 377*, 450–468.
10. Brooks, C. L., Blackler, R. J., Gerstenbruch, S., Kosma, P., Müller-Loennies, S., Brade, H., and Evans, S. V. (2008) Pseudo-symmetry and twinning in crystals of homologous antibody Fv fragments. *Acta Crystallogr., Sect. D: Biol. Crystallogr. 64*, 1250–1258.
11. Nguyen, H. P., Seto, N. O., MacKenzie, C. R., Brade, L., Kosma, P., Brade, H., and Evans, S. V. (2003) Germline antibody recognition of distinct carbohydrate epitopes. *Nat. Struct. Biol. 10*, 1019–1025.
12. Hozumi, N., and Tonegawa, S. (1976) Evidence for somatic rearrangement of immunoglobulin genes coding for variable and constant regions. *Proc. Natl. Acad. Sci. U.S.A. 73*, 3628–3632.
13. Jacob, J., Kelsoe, G., Rajewsky, K., and Weiss, U. (1991) Intraclonal generation of antibody mutants in germinal centres. *Nature 354*, 389–392.
14. Braden, B. C., and Oljak, R. J. (1995) Structural features of the reactions between antibodies and protein antigens. *FASEB J. 9*, 9–16.
15. Braden, B. C., Goldman, E. R., Mariuzza, R. A., and Poljak, R. J. (1998) Anatomy of an antibody molecule: structure, kinetics, thermodynamics and mutational studies of the antilysozyme antibody D1.3. *Immunol. Rev. 163*, 45–57.
16. Cygler, M., Rose, D. R., and Bundle, D. R. (1991) Recognition of a cell-surface oligosaccharide of pathogenic *Salmonella* by an antibody Fab fragment. *Science 253*, 442–445.
17. Jeffrey, P. D., Bajorath, J., Chang, C. Y., Yelton, D., and Hellstrom, I.; et al. (1995) The x-ray structure of an antitumour antibody in complex with antigen. *Nat. Struct. Biol. 2*, 466–471.
18. Villeneuve, S., Souchob, H., Riottot, M. M., Mazie, J. C., and Lei, P.; et al. (2000) Crystal structure of an anticarbohydrate antibody directed against *Vibrio cholerae* O1 in complex with antigen: molecular basis for serotype specificity. *Proc. Natl. Acad. Sci. U.S.A. 97*, 8433–8438.
19. Vyas, N. K., Vyas, M. C., Chervenak, M. A., Johnson, B. M., and Pinto.; et al. (2002) Molecular recognition of oligosaccharide epitopes by a monoclonal Fab specific for *Shigella flexneri* Y lipopolysaccharide: X-ray structures and thermodynamics. *Biochemistry 41*, 13575–13586.
20. van Roon, A. M., Pannu, N. S., de Vrind, J. P. M., van der Marel, G. A., van Boom, J. H., Hokke, C. H., Deelder, A. M., and Abrahams, J. P. (2004) Structure of an anti-Lewis X Fab fragment in complex with its Lewis X antigen. *Structure 12*, 1227–1236.
21. Calarese, D. A., Lee, H.-K., Huang, C.-Y., Best, M. D., Astronomo, R. D., Stanfield, R. L., Katinger, H., Burton, D. R., Wong, C.-H., and Wilson, I. A. (2005) Dissection of the carbohydrate specificity of the

broadly neutralizing anti-HIV-1 antibody 2G12. *Proc. Natl. Acad. Sci. U.S.A. 102*, 13372–13377.
22. Stähli, C., Staehelin, T., and Miggiano, V. (1983) Spleen cell analysis and optimal immunization for high-frequency production of specific hybridomas. *Methods Enzymol. 92*, 26–36.
23. Barbas III, C. F., Burton, D. R., Scott, J. K., Silverman, G. J. (2001) Phage Display: A Laboratory Manual, Cold Spring Harbor Laboratory Press, New York.
24. Brochet, X., Lefranc, M.-P., and Giudicelli, V. (2008) IMGT/V-QUEST: the highly customized and integrated system for IG and TR standardized V-J and V-D-J sequence analysis. *Nucleic Acids Res. 36*, W503–508.
25. Kosma, P., Reiter, A., Hofinger, A., Brade, L., and Brade, H. (2000) Synthesis of neoglycoproteins containing Kdo epitopes specific for *Chlamydophila psittaci* lipopolysaccharide. *J. Endotoxin Res. 6*, 57–69.
26. Kosma, P., Schulz, G., and Brade, H. (1988) Synthesis of a trisaccharide of 3-deoxy-D-*manno*-2-octulosonic acid (Kdo) related to the genus-specific lipopolysaccharide epitope of *Chlamydia*. *Carbohydr. Res. 183*, 183–199.
27. Kosma, P., Schulz, G., Unger, F. M., and Brade, H. (1989) Synthesis of trisaccharides containing 3-deoxy-D-*manno*-2-octulosonic acid residues related to the Kdo region of enterobacterial lipopolysaccharides. *Carbohydr. Res. 190*, 191–201.
28. Adamczyk, A., Moore, J. A., and Yu, Z. (2000) Application of surface plasmon resonance toward studies of low-molecular weight antigen-antibody binding interactions. *Methods 20*, 319–328.
29. McCoy, A. J., Grosse-Kunstleve, R. W., Adams, P. D., Winn, M. D., Storoni, L. C., and Read, R. J. (2007) Phaser crystallographic software. *J. Appl. Crystallogr. 40*, 658–674.
30. Collaborative Computation Project, Number 4 (1994). The CCP4 suite: programs for protein crystallography. Acta Crystallogr. *D50*, 760−763.
31. Emsley, P., and Cowtan, K. (2004) Coot: model-building tools for molecular graphics. *Acta Crystallogr., Sect. D: Biol. Crystallogr. 60*, 2126–2132.
32. Adams, P. D., Grosse-Kunstleve, R. W., Hung, L. W., Ioerger, T. R., McCoy, A. J., Moriarty, N. W., Read, R. J., Sacchettini, J. C., Sauter, N. K., and Terwilliger, T. C. (2002) PHENIX: building new software for automated crystallographic structure determination. *Acta Crystallogr., Sect. D: Biol. Crystallogr. 58*, 1948–1954.
33. Schroeder, H. W. (2006) Similarity and divergence in the development and expression of the mouse and human antibody repertoires. *Dev. Comp. Immunol. 30*, 119–135.
34. Senn, B. M., Lopez-Macias, C., Kalinke, U., Lamarre, A., Isibasi, A., Zinkernagel, R. M., and Hengartner, H. (2003) Combinatorial immunoglobulin light chain variability creates sufficient B cell diversity to mount protective antibody responses against pathogen infections. *Eur. J. Immunol. 33*, 950–961.
35. Adderson, E. E., Shackelford, P. G., Quinn, A., and Carroll, W. L. (1991) Restricted Ig H chain V gene usage in the human antibody response to *Haemophilus influenzae* type b capsular polysaccharide. *J. Immunol. 147*, 1667–1674.
36. Shaw, D. R., Kirkham, P., Schroeder, H. W., Jr., Roben, P., and Silverman, G. J. (1995) Structure−function studies of human monoclonal antibodies to *Pneumococcus* type 3 polysaccharide. *Ann. N.Y. Acad. Sci. 764*, 370–373.
37. Cadsadevall, A., and Scharff, M. D. (1991) The mouse antibody response to infection with *Cryptococcus neoformans*: VH and VL usage in polysaccharide binding antibodies. *J. Exp. Med. 174*, 151–160.
38. Pirofski, L., Lui, R., DeShaw, M., Kressel, A. B., and Zhong, Z. (1995) Analysis of human monoclonal antibodies elicited by vaccination with a *Cryptococcus neoformans* glucuronoxylomannan capsular polysaccharide vaccine. *Infect. Immun. 63*, 3005–3014.
39. Berry, J. D., Boese, D. J., Law, D. K. S., Zollinger, W. D., and Tsang, R. S. W. (2005) Molecular analysis of monoclonal antibodies to group variant capsular polysaccharide of *Neisseria meningitidis*: recurrent heavy chains and alternative light chain partners. *Mol. Immunol. 42*, 335–344.
40. Barrios, Y., Jirholt, P., and Phlin, M. (2004) Length of the antibody heavy chain complementarity determining region 3 as a specificity-determining factor. *J. Mol. Recognit. 17*, 332–338.
41. Krishnan, L., Lomash, S., Raj, B. P. J., Kaur, K. J., and Salunke, D. M. (2007) Paratope plasticity in diverse modes facilitates molecular mimicry in antibody response. *J. Immunol. 178*, 7923–7931.
42. Xu, J. L., and Davis, M. M. (2000) Diversity in the CDR3 region of V_H is sufficient for most antibody specificities. *Immunol. 13*, 37–45.
43. Brade, H., and Rietschel, E. T. (1984) α2→4-Interlinked 3-deoxy-D-*manno*-octulosonic acid disaccharide. A common constituent of enterobacterial lipopolysaccharides. *Eur. J. Biochem. 145*, 231–236.
44. Kabat, E. A., Wu, T. T., Bilofsky, H., Reid-Miller, M., Perry, H. (1983) Sequence of Proteins of Immunological Interest, National Institutes of Health, Bethesda, MD.
45. Abhinandan, K. R., and Martin, A. C. R. (2008) Analysis and improvements to Kabat and structurally correct numbering of antibody variable domains. *Mol. Immunol. 45*, 3832–3839.